

Geometry attained by pressurized membranes

A. Palisoc^{*}, G. Veal^{*}, C. Cassapakis^{*}, G. Greschik[†], M. Mikulas[†]

L'Garde, Inc., Tustin, CA*

Center for Aerospace Structures
University of Colorado, Boulder, CO[†]

ABSTRACT

An intensive investigation has been carried out to study the surface profiles obtained as a result of the large deformations of pressurized membranes. The study shows that the inflated membrane shapes may have the requisite surface accuracy for use in future large space apertures. Both analytical and experimental work have been carried out. On the analytical side, the classical work of Hencky on flat circular membranes was extended to eliminate the limitations it imposed; namely a lateral non-follower pressure with no pre-stress. The result is a computer program for the solution of the pressurized circular membrane problem.[5] The reliability of the computer program is demonstrated via verification against FAIM, a nonlinear finite element solver developed primarily for the analysis of inflated membrane shapes. The experimental work includes observations made by Veal[11] on the (W-shaped) deviations between the membrane deflected shape and the predicted profile. More recent measurements have been made of the deformations of pressurized flat circular and parabolic membranes using photogrammetric techniques. The surface error quantification analyses include the effect of material properties, geometric properties (effect of seams), loading uncertainties, and boundary conditions. These effects are very easily handled by the special FEM ccFAIM which had recently been enhanced to predict the on-orbit dynamics, RF, and solar concentration characteristics of inflatable parabolic antennas/reflectors such as the IAE (Inflatable Antenna Experiment) that flew off the space shuttle Endeavour in May 1996. The results of measurements have been compared with analyses and their ramifications on precision-shape, large-aperture parabolic space reflectors are discussed. Results show that very large space apertures with surface slope error accuracies on the order of 1 milliradian or less are feasible. Surface shape accuracies of less than 1 mm RMS have been attained on ground measurements.

Keywords: inflatable, antenna, reflector, membrane, finite element

INTRODUCTION

There is a need for large aperture space telescopes in the future. Current technology precludes the space deployment of very large aperture devices because of weight and volume constraints. Due to their very low weight and low, conformable packaged volume, inflatable reflectors may be the answer. If inflatables can be made to work as large reflectors in space, they will provide cost-effective solutions for a variety of needs including very large solar collectors, solar concentrators, mm-wave antennas, and Space Very Long Baseline Interferometry (SVLBI) systems, to name a few. In fact, because of greatly reduced launch costs, the use of inflatable reflectors for antennas or solar concentrators can make possible important missions that otherwise would just be economically prohibitive. On May 20th, 1996, the Space Shuttle Endeavour launched the first ever inflatable space antenna (14m diameter) called the Inflatable Antenna Experiment (IAE).

The Space VLBI missions involving apertures larger than 20 meters will be prohibitive because of launch cost. Space VLBI is useful because of the potential of synthesizing a gigantic space telescope with a diameter several times the size of the earth. At this size and at centimeter radio wavelengths, the resolution is about 30 microarcseconds – 10 times better than can be achieved using ground VLBI alone and almost 1000 times finer than can be achieved with the Hubble Space Telescope at optical wavelengths. Large, accurate aperture diameters greater than 20 meters is feasible with the use of inflated membrane shapes. Its accuracy can be further increased with the use of adaptive feeds and optics. The support structure of such a system is in itself also an inflatable but rigidizes after deployment. Only the lenticular structure is purely inflatable. Aperture diameters between 50 m and 100m for use in a space-based system like the Terrestrial Planet Finder and the Terrestrial Planet Imager will be impossible without the use of very lightweight, and volume-conformable systems. One other advantage of an inflatable system is its inherent high damping characteristics. Typical structural damping coefficients are between 5% and 20%. [1]

To be of practical interest, space-based large inflatable apertures for use in astronomical observations, must operate at frequencies upwards from 20 GHz. For a 28 GHz antenna (wavelength $\lambda = 10.7$ mm), a 2 dB loss of antenna gain G/G_0 – according to reference [12] $G/G_0 = \exp[-(4\pi\sigma_{RMS}/\lambda)^2]$ – corresponds to an RMS error of $\sigma_{RMS} = (0.2 \ln 10)^{1/2} \lambda / (4\pi) = 0.58$ mm.

Probably the issue of greatest concern for inflatable space systems is the possibility of meteoroid puncture. This prompted NASA to turn early on to self-rigidizing systems so that inflation was used mainly as a forming erection mechanism. Many of the advantages of space inflatables such as ruggedness, damped dynamics, and low-weight were lost by this. It has been shown that the meteoroid problem was grossly overestimated and that inflatable systems can remain operating for ten or more years by replacing the lost inflatant while maintaining a low total system weight. [2] The makeup inflatant weight is only a small fraction of the total system weight.

Ground measurements have yielded surface shape accuracies between 0.67 mm and 1.3 mm RMS for gored 3-meter-diameter systems with 0.8 mm to 0.96 mm as typical values. This is the RMS deviation of the measured surface from a best-fit paraboloid. A surface accuracy of 1.3 mm RMS was achieved on a 7 meter, 0.5F/D inflatable parabolic reflector. Measurements also show that surface slope errors of 1 milliradian or less are feasible. It must be noted that these surface accuracies and surface slopes were achieved using off-the-shelf materials with the reflector formed from flat gores. Figure 1 shows one of the first 3 meter reflectors built by L'Garde. The surface was measured using a scanning laser system and yielded a surface accuracy of 1.12 mm RMS. [11] Although inflatable reflectors using current technology do not have the required accuracy for use as space telescopes, we believe that the enabling technologies such as improved material properties, better material uniformity, and greatly-improved manufacturing processes are in the very near future. At present, inflatable reflectors are fabricated using flat gores joined together at the seams. The use of doubly curved gores will yield better accuracy but the process becomes expensive for larger diameters. However, the cost is not necessarily prohibitive.

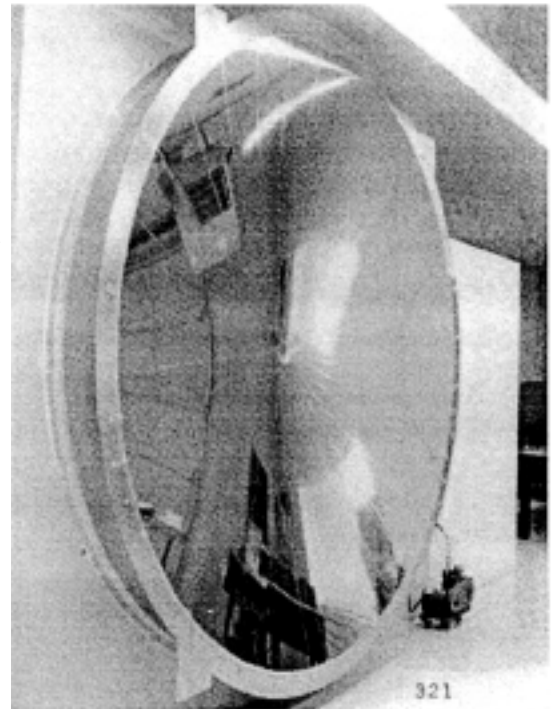


Figure 1. An early 3-meter diameter inflatable reflector

In this paper, we present the results of our analytical work and the validation of its predictions against experimental measurements. The objective of this paper is to show the feasibility of using inflated membrane shapes as telescope mirrors and to validate against experimental results, the analytical codes used in the calculation of the geometry attained by pressurized membranes. This validation is critical as these tools will be used in a more intensive study of inflated membranes to assess their surface shape accuracy for use as mirrors for antennas and telescopes. The experimental setup consists of a thin sheet of material of precisely known prestress and clamped at its edge to form a flat circular membrane.

ANALYTICAL AND NUMERICAL SOLUTIONS

In order to address the issues concerning the surface accuracies of inflatables, a set of analytical tools capable of accurate shape prediction is critical. For pressurized membranes, numerical analysis can be troublesome and closed form solutions exist only for the simplest of configurations. If an exact solution exists, it may not be in closed form and thereby require numerical methods. This provided the impetus to develop the analytical tools discussed in this paper.

FAIM, a problem-dependent material and geometric nonlinear finite element computer program for the analysis of membrane structures was developed to study and predict the large deflection of inflatable structures. [3] It has nonlinear material capability and accepts various types of loadings and boundary conditions. More recently, *AM*, a high precision analysis code for axisymmetric membranes capable of modeling wrinkling was developed. [5,6] Its accuracy and precision are such that it is applicable upwards to optical frequencies. The initial validations of both *FAIM* and *AM* were carried out by comparing its results against the Hencky [7] solution, namely the deflection of a flat circular membrane due to a lateral load. Another validation test

case used for FAIM was the solution of the *inverse problem*; i.e., what must be the initial uninflated shape given the desired final shape, loading condition and material properties.[4] The same capability was included in the axisymmetric membrane code, *AM*. [5,6]

A number of authors have done analytical work on membrane deflection problems as a result of applied loads, dating back to the classic paper by Hencky on the profile attained by a flat circular membrane subjected to a lateral load.[7] This and subsequent work that includes extending Hencky's original work are in general restricted to an initially flat circular membrane. Approximations need to be made in order to render the problem exactly solvable, although the solution sometimes involve numerical methods.[8,9] The code *AM* on the other hand solves the exact differential equations without approximations or linearizations of the equations.[5,6] It uses the finite difference technique. For the governing equations, the interested reader is referred to references [5] to [10].

DEFLECTIONS OF THE FLAT CIRCULAR MEMBRANE

The deflections of an initially flat circular membrane may be used to approximate a paraboloid of revolution. Table 1 is taken from reference [5]. It shows the best-fit parabola *F/D* ratio and *RMS errors*[†] for a deflected 3-meter-diameter circular membrane. The load cases 125, 250, 500, and 1000 refer to the membrane film stress *inpsi*. Table 2 lists the parameters used. As shown in reference [5], an added *prestress* in the flat membrane decreases the RMS errors and flattens the shape; i.e., lengthens the focal length.

TABLE 1a. RMS ERRORS AND *F/D* RATIO FOR BEST-FIT PARABOLOID

Load Case	125	250	500	1000
σ_{cr} [Mpa]	0.8618	1.7240	3.447	0.895
<i>F/D</i>	10.1	7.13	5.04	3.56
ϵ_{RMS} [mm]	0.178	0.251	0.356	0.507

TABLE 1b. RMS ERRORS AND *F/D* RATIO FOR BEST-FIT PARABOLOID (Pre-stress 340 psi)

Load Case	125	250	500	1000
σ_{cr} [Mpa]	2.445	2.860	4.28 1	7.589
<i>F/D</i>	32	13	6.65	4.06
ϵ_{RMS} [mm]	0.002	0.024	0.123	0.300

TABLE 2. PARAMETERS OF CIRCULAR MEMBRANE

Material	Kapton
Thickness, t	0.0127 mm (0.5 mil)
Young's Modulus, E	5.516 Gpa (800 ksi)
Poisson's Ratio, ν	0.3
CTE	$1.2 \times 10^{-5} \text{ C}^{-1}$
Diameter	3.00 m

[†] The RMS error is taken as the RMS of the path length change due to deviations of an otherwise perfect surface according $\epsilon_{RMS} = [\int (\Delta l)^2 dA/A]^{1/2}$.

Figure 2 is a plot of the RMS errors for the 3m diameter flat membrane as a function of circular area considered. (Both linear and logarithmic plots shown.) For example, if only the 2m inner diameter is considered (radial distance = 1.00 meter) the RMS errors are, respectively, 0.028 mm, 0.039 mm, 0.055 mm, and 0.08 mm for the 125, 250, 500, and 1000 psi load cases. The main reason why this approach is impractical for forming approximate parabolic shapes for space telescopes is the long F/D ratio and the high skin stresses ($\sigma > 300$ psi). The longer the F/D ratio, the longer the booms are to the feed location - added weight to the total system mass. On top of this, higher skin stresses mean higher inflation pressures translating to higher makeup gas weights to replenish that lost to meteoroid puncture. Work is on-going to reduce the overall system weight with the use of low-modulus materials for the film membrane. For a given inflation pressure, a shorter F/D ratio and lower skin stress are achieved with a low-modulus membrane.

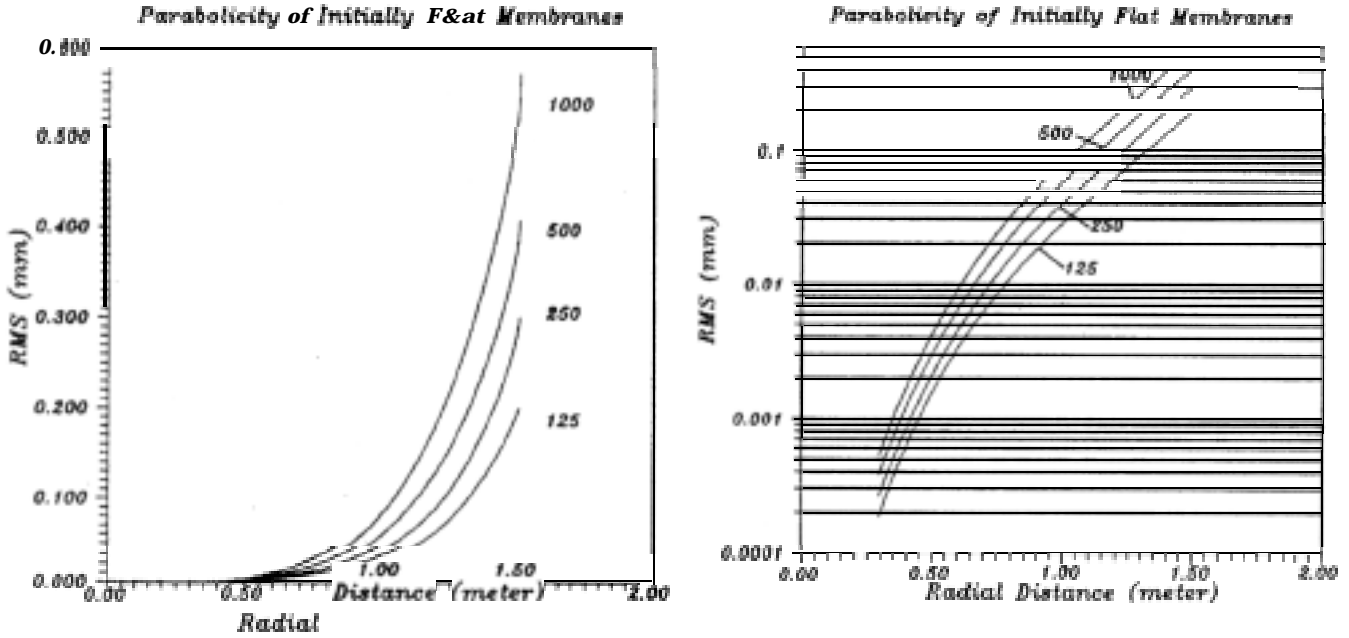


Figure 2. Parabolicity of 3-meter-diameter circular membrane for different circular areas

PRESSURIZING MEMBRANES TO PARABOLIC SHAPES

The inverse problem

The success or failure of inflatable reflectors is directly tied to their ability to maintain a smooth parabolic shape. One of the major issues that must be solved is what is commonly referred to as the inverse problem: what must be the initial shape of an inflatable shell membrane such that it attains a smooth parabolic surface after experiencing large structural deformations? The solution to this is used in the construction of inflatable reflectors even for initially flat gores.[4] This feature is also included in code *AM*. [5,6] The earliest validation of code *FAIM* consisted of comparing its results on the deflections of membrane problems (obeying the inverse problem) to perfect parabolic shapes. Figure 3 shows the *FAIM* predictions of the deflections of three different initial shapes ($\nu = 0.1, 0.3, 0.45$) to the same final parabolic surface. The (numerical) *FAIM* results as well as *AM*, agree with the analytical solution to 6 decimal places. The results are expressed in terms of the dimensionless parameters $(z/2F)$ and $(r/2F)$ where F is the focal length, z is the vertical displacements, and r is the radial distance from the vertex. The case shown in Fig. 3 is for a very large deformation case - $pF/(E_t) = 1$.

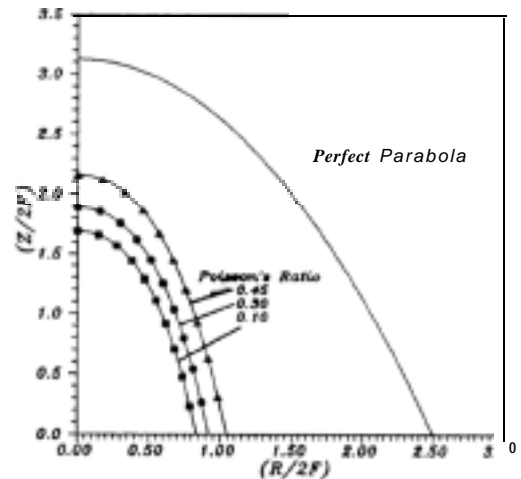


Figure 3. Comparison of exact paraboloid with *FAIM*-calculated inflated shapes

Reflectors using flat gores

Most of the inflatable reflectors that have been fabricated to date have been formed using gores which, prior to any inflation pressure, curve only in the meridional direction. The curvature in the circumferential or hoop direction is provided by the inflation pressure. The main reason for fabricating inflatable reflectors this way is its simplicity thereby reducing cost. The gores are visible in the reflector shown in Fig. 1. A 3-meter 14-gore offset inflatable reflector built as a sector of the IAE 14-meter-diameter antenna is shown in Fig. 4. The “dots” are retroreflective targets used for measuring the surface profile using photogrammetry. The surface RMS deviation of this reflector from the best-fit paraboloid was 0.67 mm RMS. The reflector was fabricated using 0.25mil aluminized mylar.

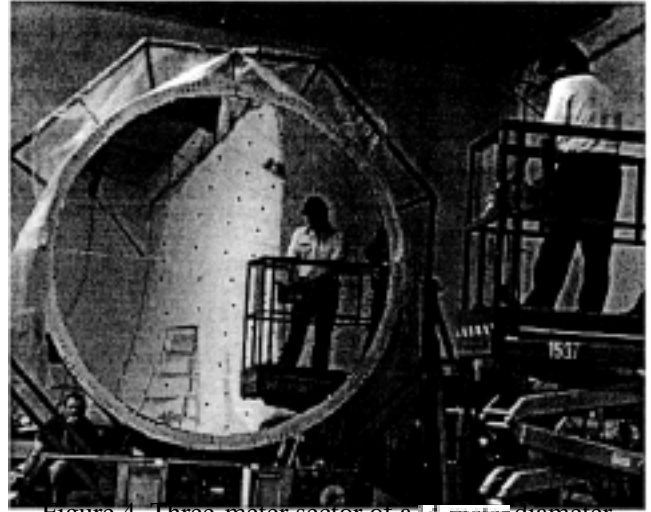


Figure 4. Three-meter sector of a 14-meter diameter offset reflector

The surface accuracy calculated using flat gores (in *FAIM*) to form a doubly curved inflatable membrane reflector is shown in Fig. 5 where we plot for both a 3-meter and a 7-meter diameter with an $F/D = 1/2$ and 1. The load case considered is the $\sigma = 250$ psi case. The seam tape used in the simulation is 0.25 mil thick, 0.35 inch wide with $E_{seam} = 1000$ psi. At this skin stress level, the inflation pressure required for the 3m diameter is 0.00212 psi and 0.00106 psi for a $F/D = 1/2$ and 1, respectively. For a 7 m diameter, the inflation pressure is 9.07×10^{-4} psi and 4.5×10^{-4} psi for $F/D = 1$ and $1/2$, respectively. These pressures are equivalent, respectively to $1/16000^{\text{th}}$ and $1/32400^{\text{th}}$ of an atmosphere. For an $F/D = 1$, 25 meter diameter reflector operating at the same skin stress of

$\sigma = 250$ psi, the inflation pressure is only $1/115,748^{\text{th}}$ of an atmosphere. These very low inflation pressures help in reducing the makeup gas weight requirement.

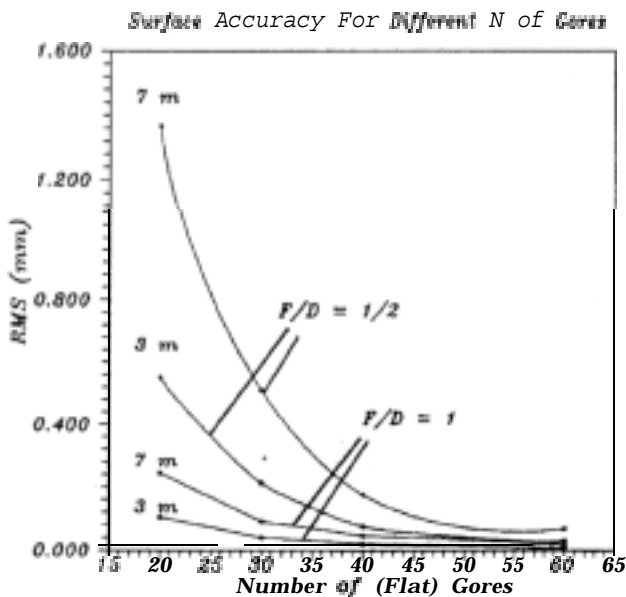


Figure 5. Reflector surface accuracy dependence on number of (flat) gores used. ($F/D = 1/2, 1$) $E_{seam} = 1000$ psi, $P = 0.5$ mil, $\sigma = 250$ psi

Notice in Fig. 5 how the surface accuracy improves as the number of gores increases and for the two cases considered, no significant improvement is achieved beyond 60 gores. It must also be noted that the reflector flattens as the number of gores decrease, i.e., the focal length is slightly increased.

Figure 6 ($F/D = 1/2, 1$) shows the improvement in the surface accuracy as a function of the circular area considered. This is similar to Fig. 2 for the flat membrane. The reason for the improvement in the surface accuracy as the circular area is decreased is due to the fact that the integrated deviation between the flat gore and the curved parabolic surface is less at smaller radii. Note that the surface accuracy remains fairly constant for most of the region considered until it gets to about 80% to 90% of the aperture radius where the curves suddenly experience a large change in slope.

To assess the effect of edge mounting on the resulting parabolic shapes using flat reflector gores, code *FAIM* was used for the cases where the gore length was given an error of $\pm \Delta L$ as shown

in Fig. 7. A negative ΔL corresponds to a gore that was made shorter than the design length and a positive ΔL corresponds to a longer gore. A shorter gore results in a longer effective focal length and a longer one results in a deeper dish and thereby, a shorter focal distance.

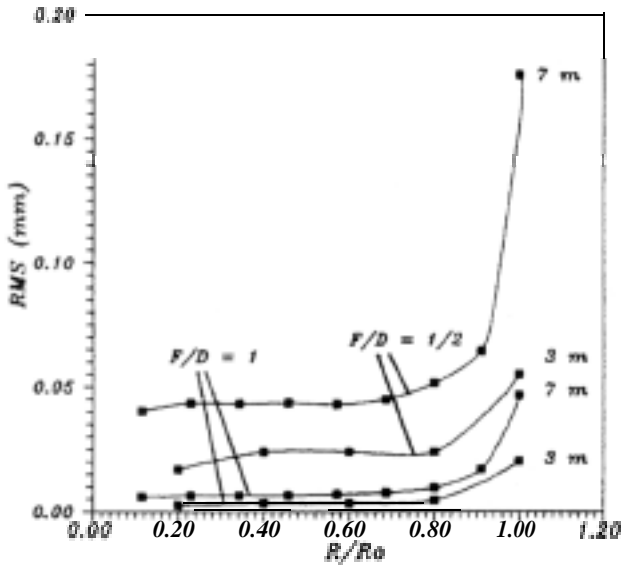


Figure 6. Reflector surface accuracy for different circular regions. ($F/D=1/2$) $E=500$ ksi, $E_{tape}=1000$ psi, $t=0.5$ mil, $\sigma=250$ psi, $R_0=1.5$ m for 3m -diameter and $R_0=3.5$ m for 7m-diameter. Number of gores is 40 for either case.

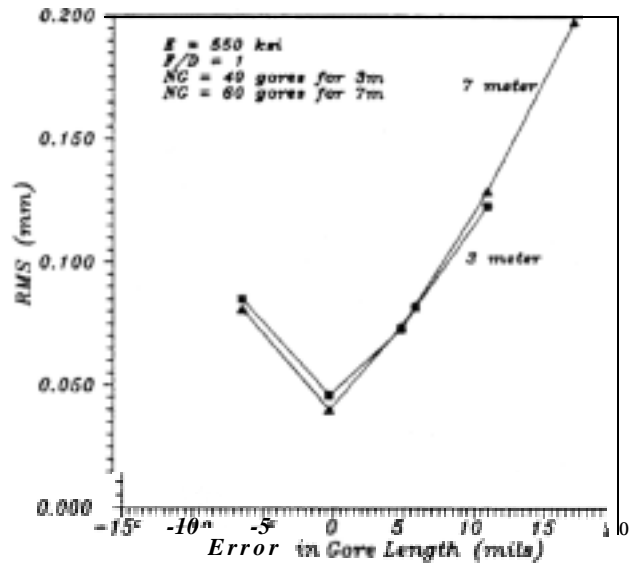


Figure 7. Effect of longer and shorter gores

Reflectors using preformed membranes

A few runs using *FAIM* were made to look at the magnitudes of reflector accuracy using gores with the same (double) curvature as the initial uninflated shape obtained from the solution of the *inverse problem*. In practice, doubly-curved gores are obtained by thermo-forming where the membrane is heated to a high temperature while pressed on a mandrel with the desired double curvature. However, we do not expect the formed reflector to inflate to the perfect parabolic shape because in practice, especially for large diameters, the reflector can be formed only by seaming together the doubly-curved gores using a tape material. Figure 8 shows the resulting reflector surface accuracy obtained using two different seam tape materials, $E_{tape1} = 500,000$ psi and $E_{tape2} = 1000$ psi. The load case considered for both cases is the $\sigma=250$ psi case.

Figure 8 shows that increasing the number of “gores” degrades the surface quality. This behavior is opposite that shown in Fig. 5 (as expected). The overall surface accuracy for the case of an initially doubly-curved surface is better than that of initially flat gores.

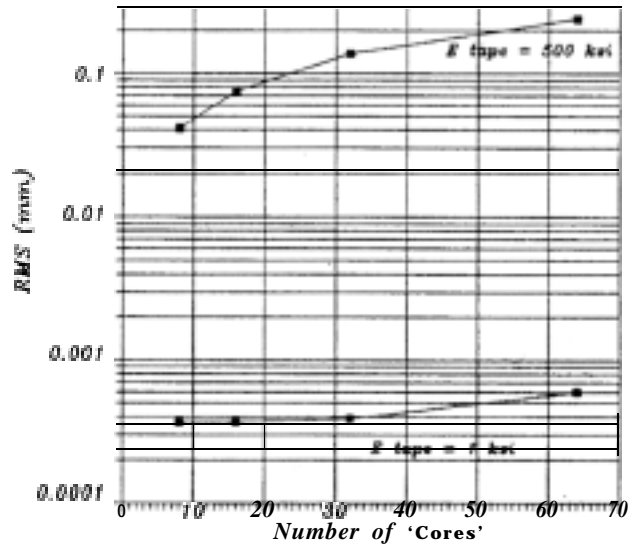


Figure 8. 3 meter reflector formed using doubly-curved gores. $F/D=1$, $E_{tape1}=500$ ksi, $E_{tape2} = 1000$ psi

Measurement results of the deflection of flat circular membrane

In this section, we present the results of the correlation of the results of our analytical codes and measurements of the surface profile of initially prestressed circular membranes. Since it is easier to achieve and control a finite, *nonzero* initial prestress state in a membrane than an initial zero stress condition, the membranes used in the experiment were given an initial prestress of 50psi. Table 3 lists the parameters of two circular membranes used in the tests.

TABLE 3. PARAMETERS OF THE 1.0-METER CIRCULAR MEMBRANES USED FOR TEST [13]

Material	Kapton, Isotropic	Mylar, 30°, Orthotropic
Thickness	0.0005 inch	0.0005 inch
Measured Modulus	543,000 psi	$E_1=937000$ psi, $E_2=649000$ psi
Poisson's Ratio	0.3	$\nu_{12} = 0.35$ $\nu_{21} = 0.24$
Diameter	1.0 meter	1.0 meter
Prestress	50 psi	50 psi

The Young's modulus and Poisson's ratios were measured [13] using a video metrology system. The values shown in Table 3 are average results. While kapton is believed to be isotropic, mylar is orthotropic with principal material axes approximately 30° from the material transverse (T) direction as shown in Fig.9. The details of the measurement method are discussed in reference [13]. Figure 10 shows a polar plot of the measured modulus of Mylar.

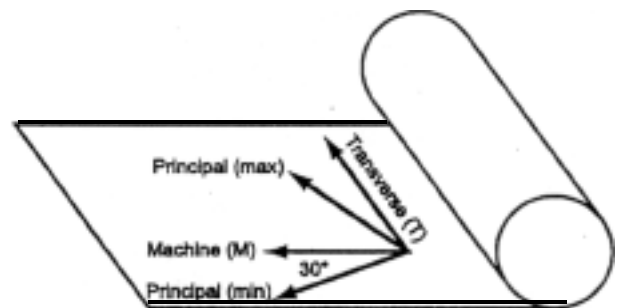


Figure 9. Definition of machine (M) and transverse (T) material directions and the principal material axes for mylar

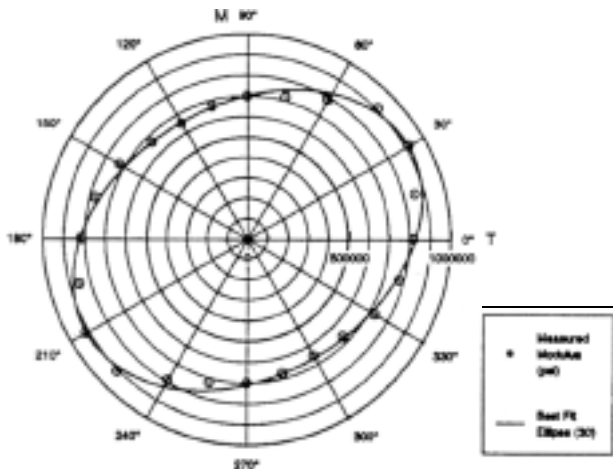


Figure 10. Experimental determination of Mylar principal axes orientation using one dimensional tensile tests. The ellipse is oriented at 30° relative to the transverse direction

Each membrane was prestressed to 50 psi before it was bonded and clamped to a 1 meter (inner) diameter aluminum ring. The membrane was subjected to an isotensoid stress state by a method suggested in reference [14]. Figure 11 is a photograph of the circular membrane where one can clearly see the retroreflective targets used by the videogrammetry measurement system (VSTARS). [15] The measurement system has an accuracy of 0.0001 inch.

The result for mylar is shown in Fig. 12 for inflation pressures of 0.0017 psi and 0.013 psi, respectively. These correspond to skin stresses at the center of 636 and 3076 psi, respectively. The predictions by *FAIM* is superimposed on the same plot. The error bars correspond to the uncertainties in the measurement of the inflation pressure and the nonuniformity of the modulus over the material surface. However, a 10% higher (or lower) modulus value corresponds to only a 3% decrease (or increase) in the vertical deflection of the membrane. For mylar, the uncertainty in the modulus is +10%, -5% and for kapton, it is ±6%. Notice the excellent agreement between *FAIM* and experiments especially for mylar. The agreement is not as good for kapton (Fig. 13) but it is still within experimental error. The reason for this is that, the kapton material used was not as "flat" as the mylar. In fact, even after the kapton was stretched to achieve a 50 psi prestress, certain sections of the kapton showed minor rippling. This is believed to have existed in the material as a result of

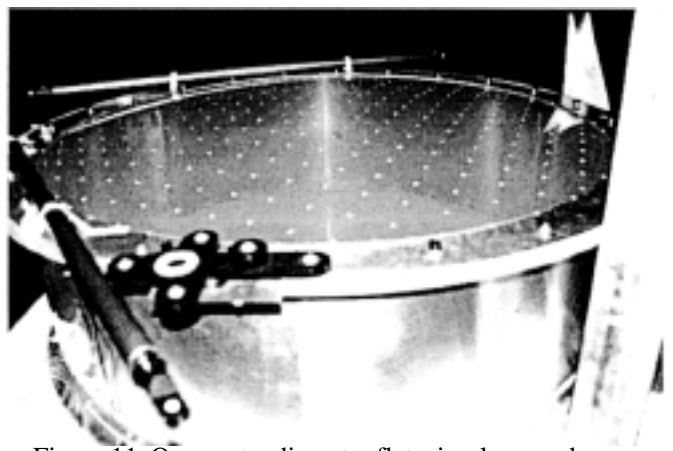


Figure 11. One-meter diameter flat, circular membrane

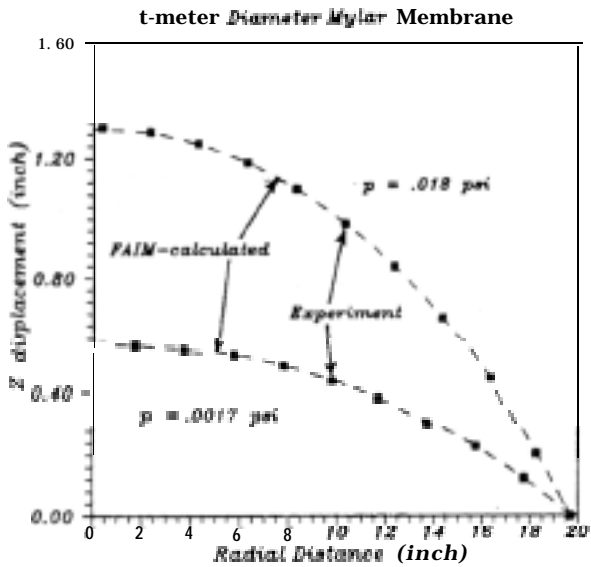


Figure 12. Measured mylar profile. Inflation pressure = 0.0017psi, 0.018psi ($\sigma = 636\text{psi}, 3076\text{psi}$)

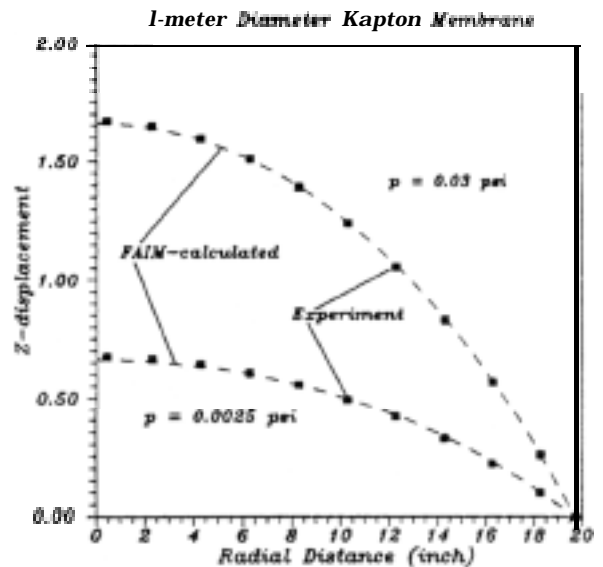


Figure 13. Measured Kapton profile. Inflation pressure = 0.0025psi, 0.030psi ($\sigma = 668\text{psi}, 4000\text{psi}$)

manufacturing. There are other types of Kapton, such as Kapton E that exhibit far more uniformity than the kapton HN type used. We could not use kapton E because at the time the experiment was performed, it was not available in the right width dimension.

During the test, after pressurizing to 0.0017psi and then to 0.018psi, the pressure was set back to 0.0017psi and a second measurement of the surface was made at this lower pressure to check whether or not the membrane had yielded. The check measurement shows the same surface profile within the videogrammetry system's accuracy and precision.

The displacement contours from the measurement of mylar is shown in Fig. 14. It is hard to see the "elliptical" contour with the "unaided eye." When this was analyzed using a best-fit ellipse program, the results show that the best-fit ellipse is oriented at about 40° from the transverse direction. The predicted contours by FAIM likewise shows an ellipse of low "ellipticity" - Fig. 15. The "jaggedness" in Fig. 14 is an artifact of the plotting program used.

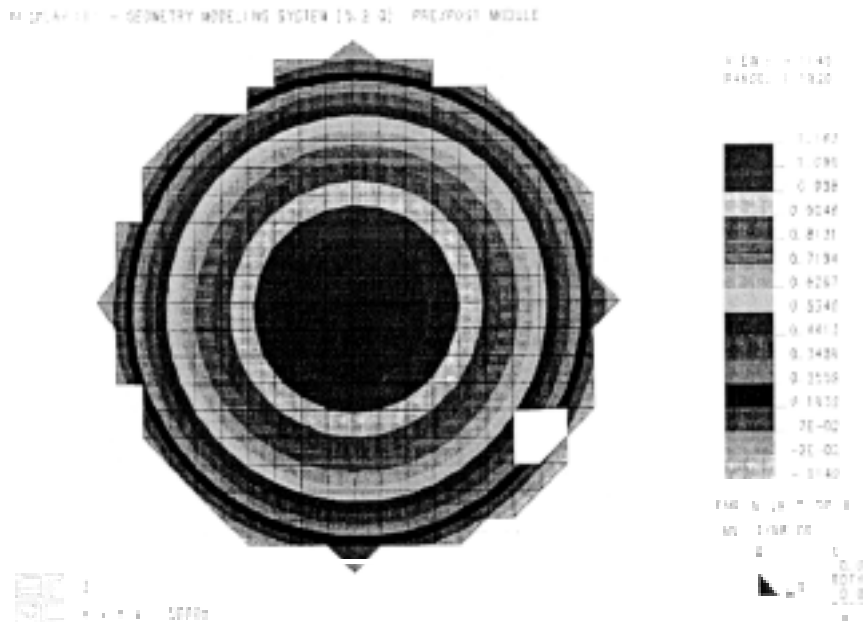


Figure 14. Contour plot of measured surface of mylar

The surface accuracy of reflectors made out of initially flat gores may be increased by exploiting the fact that edge effects extend only to the vicinity of the perimeter. A much higher surface accuracy is achieved by not including (metalizing) this outer region. The central portion of the reflector essentially remains unchanged and only displaces vertically. A movable as well as an adaptive feed system will further enhance its performance. A lower modulus material will also help advance the technology further by bringing the make-up gas requirement even lower. A low modulus material also means that the skin stress required to remove the packaging wrinkles is also lowered.

Although inflatable reflectors do not currently have the surface accuracy required for use as space telescopes, we believe that the enabling technologies such as improved material properties, better material uniformity, greatly-improved manufacturing process, and low-material moduli are in the very near future. A roadmap to the technology had been prepared by L'Garde with input from JPL and Phillips Laboratory and work on improving the accuracy of precision inflatable space structures is actively going on.

Acknowledgement

We would like to thank Lt. Jonathan Bishop of Phillips Laboratory for letting us use the VSTARS Videogrammetric Measurement System for the experimental studies. Some of the work presented in this paper has been supported by Contract No. F29601-96-C-0131 from the U.S. Air Force, Phillips Laboratory to study Large Inflatable Structures (LIS). The addition of nonlinear material capability to code FAIM was supported by NASA/JPL Contracts NAS7-1219 and NAS7-1313. The experimental measurement of the deflections of the flat circular membranes was supported by Contract No. 960318 Task L with NASA/JPL on the New Millennium Program. We also thank Yuli Huang of L'Garde for running most of the FAIM calculations presented in this paper, as well as for writing the code to extract the best-fit ellipse from the measured surface contours.

References

1. Palisoc, A.L., Inflatable Reflector Development Program, Task 3 Report, L'Garde Technical Report LTR-94-AP-008, May 1994.
2. Thomas, M. and Friese, G., "Pressurized Antennas for Space Radars", AIAA paper 80-1928-CP, AIAA Sensor Systems for the 80's Conference, December 1980.
3. Palisoc, A.L. and Huang Y., "Design Tool for Inflatable Space Structures", In 38th AIAA/ASME/ASCE/AHS/ASC Structures, Structural Dynamics and Materials Conference, pp. 2922-2930, Kissimmee, FL, April 7-10, 1997. AIAA-97-1378.
4. Thomas, M., "Effect of Inflation Pressure on Paraboloid Structure", L'Garde Memorandum, LM-79-MT-054, August 10, 1979.
5. Greschik, G., Palisoc, A., Cassapakis, C., Veal, G., and Mikulas, M., "Approximating Paraboloids with Axisymmetric Pressurized Membranes", In 39th AIAA/ASME/ASCE/AHS/ASC Structures, Structural Dynamics, and Materials Conference, Long Beach, CA, April 1998.
6. Greschik, G., Mikulas, M., and Palisoc, A., "Approximation and Errors in Pressurized Axisymmetric Membrane Shape Predictions", In 39th AIAA/ASME/ASCE/AHS/ASC Structures, Structural Dynamics, and Materials Conference, Long Beach, CA, April 1998.
7. Hencky, H., *Über den Spannungszustand in kreisrunden platten mit verschwindender Biegesteifigkeit* *Zeitschrift für Mathematik und Physik*, 63: 3 11-3 17, 19 15.
8. Campbell J.D., On the theory of initially tensioned circular membrane subjected to uniform pressure. *The Quarterly Journal of Mechanics and Applied Mathematics* IX(): 84-93, 1956.

9. Fichter, W.B., Some solutions for the large deflections of uniformly loaded circular membranes. NASA Technical Paper 3588, NASA Langley Research Center, Hampton, VA, July 1997.
10. Green A.E. and Adkins J.E., Large Elastic Deformations, Clarendon Press, Oxford 1970.
11. Veal, G., "Highly Accurate Inflatable Reflectors, Phase II", Final Report for AFRL, L'Garde Technical Report LTR-86-GV-129, March 1987.
12. Ruze, J., "Antenna Tolerance Theory - a review", Proc. Of the IEEE, 54(4):633-640, April 1966.
13. Murphey, T. and Mikulas, M., "Measurement of Elastic Constants for 0.0005 inch thick Mylar and Kapton Films", Center for Space Construction, University of Colorado at Boulder, Feb. 5, 1998.
14. Mikulas, M., Center for Space Construction, University of Colorado at Boulder, private communication, Nov. 1997.
15. VSTARS, Videogrammetric Measurement System, VSTARS, by GSI, Corp., Melbourne, FL.